Journal of Applied Mathematics and Physics, 2024, 12, 2333-2345
https://www.scirp.org/journal/jamp
ISSN Online: 2327-4379
ISSN Print: 2327-4352

Sound Transmission Loss Analysis of a Double Plate-Acoustic Cavity Coupling System with In-Plane Functionally Graded Materials

Changzhong Chen, Mingfei Chen, Wenliang Yu

School of Mechanical Engineering, Guizhou University, Guiyang, China
Email: czchengzu@outlook.com

How to cite this paper: Chen, C.Z., Chen, M.F. and Yu, W.L. (2024) Sound Transmission Loss Analysis of a Double Plate-Acoustic Cavity Coupling System with In-Plane Functionally Graded Materials. *Journal of Applied Mathematics and Physics*, **12**, 2333-2345.
https://doi.org/10.4236/jamp.2024.126139

Received: April 28, 2024
Accepted: June 25, 2024
Published: June 28, 2024

Abstract

In this paper, the isogeometric analysis (IGA) is employed to develop an acoustic radiation model for a double plate-acoustic cavity coupling system, with a focus on analyzing the sound transmission loss (STL). The functionally graded (FG) plate exhibits a different material properties in-plane, and the power-law rule is adopted as the governing principle for material mixing. To validate the harmonic response and demonstrate the accuracy and convergence of the isogeometric modeling, ANASYS is utilized to compare with numerical examples. A plane wave serves as the acoustic excitation, and the Rayleigh integral is applied to discretize the radiated plate. The STL results are compared with the literature, confirming the reliability of the coupling system. Finally, the investigation is conducted to study impact of cavity depth and power-law parameter on the STL.

Keywords

Isogeometric Analysis, Sound Transmission Loss, Double-Plate System, Functionally Graded Materials, Acoustic Structure Coupling

1. Introduction

Double-plate system is a commonly used sound insulation structure, which is widely used in engineering and life. However, the coupling characteristics between the plates and the acoustic cavity of the double-plate system will affect the sound insulation ability. Functionally graded materials (FGMs) are currently highly popular and useful materials, as they possess exceptional heat resistance and mechanical properties. With the widespread use of FGMs, FGMs will appear in double-plate system. Therefore, studying the STL of the system with in-plane FGMs has important engineering value for acoustic design and noise control of

engineering and machinery.

Researchers have begun to study the double-plate system very early, and have done a lot of research [1]-[4] on the system in theory and experiment. Based on these literatures, it is not difficult to see that the research is basically focused on homogeneous materials, and now under the industrial background of large-scale application of composite materials, the acoustic radiation characteristics of anisotropic composite such as FGMs have attracted the attention of researchers. Chandra *et al.* [5] studied the vibro-acoustic characteristics and STL of FG plates using the first-order shear deformation theory and the power-law rule, and obtained the effect of the volume fraction of the constituent material on the transmission efficiency. In addition, they [6] also proposed an improved model of the near-field element radiator method to study the acoustic radiation and transmission characteristics of FG plates. Three-dimensional elasticity theory was applied firstly by Yang *et al.* [7] to investigate the acoustic radiation of FG plates. In their next study, they [8] supplemented the acoustic radiation study of FG plates in a thermal environment, and conclusion showed that temperature has a significant effect on the acoustic radiation characteristics. Isaac *et al.* [9] studied the vibro-acoustic behavior of functionally graded lightweight square plate (FGLSP) under different boundaries; through analysis and experiments, it was proved that FGLSP was better than homogeneous materials. Fu *et al.* [10] applied Reddy's high-order shear deformation theory to study the radiation efficiency of laminated FG carbon nanotube reinforced composite plates. The hyperbolic shear deformation theory (HSDT) was presented by Talebitooti *et al.* [11] to study the STL of FG plates. Based on the FGMs acoustic window of the simplified sonar dome model, Li *et al.* [12] optimized the STL of FGMs acoustic window through double Fourier transform and wavenumber spectrum analysis to suppress noise. The multi-layer plate (MLP) transfer function method and the wavenumber-frequency spectrum of turbulent fluctuating pressure were used by Zhou *et al.* [13] to study the STL of multi-layer FGMs acoustic window excited by external turbulence. Drawing from the aforementioned literatures, the parameters of the FG plates can affect the STL of the system and adjust the appropriate parameters that is great significance for noise control.

IGA can avoid the errors caused by the interaction between CAD and CAE. In the collected literatures [14]-[18], IGA has good adaptability and accuracy to FGMs and acoustic structure coupling system. As far as the author knows, the research on the STL of the double plate-acoustic cavity coupling system with in-plane FGMs is limited. Inspired by these, we use IGA to establish acoustic radiation model to study the STL of the system. The accuracy and convergence are verified using ANASYS and published literature. The influence of the power-law parameter and cavity depth on the STL is studied.

2. Theoretical Formulas

2.1. Acoustic Radiation Model

Figure 1 is a schematic diagram of the acoustic radiation model of the double

plate-cavity coupling system with in-plane FGMs. The plane wave with tilt angle φ and azimuth angle θ is incident on the upper plate. Some of the wave radiated from the lower plate through the acoustic cavity or reflected from the upper plate. According to the model, the STL of the coupling system is studied. A unit force F is applied on the upper plate to obtain the response of the system.

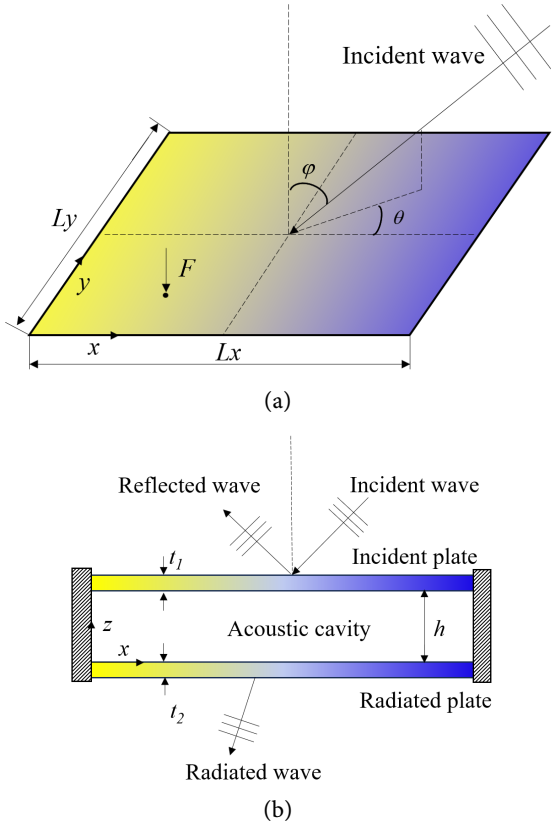

Figure 1. Acoustic radiation model of double plate-cavity coupling system with in-plane functionally graded materials. (a) The top view; (b) The side view.

The material of the FG plates is formed by mixing two materials according to the volume fraction. The material properties of FGMs change smoothly from one side to the other side. The uniform change of the two colors in **Figure 1** can represent the material properties and properties of the material in the in-plane gradient change, and the material properties meet the following equations:

$$V_e = \left(\frac{x}{L_x}\right)^{k_x} \tag{1}$$

$$V_m = 1 - V_e \tag{2}$$

$$\begin{cases} E = E_m V_m + E_e V_e \\ \rho = \rho_m V_m + \rho_e V_e \\ \mu = \mu_m V_m + \mu_e V_e \end{cases} \tag{3}$$

where k_x is the power-law parameter; e and m are aluminum alloy and ceramic; E, ρ and μ are Young's modulus, density and Poisson's ratio respectively.

2.2. Isogeometric Analysis

IGA is a new numerical method based on splines function. The commonly used spline functions are non-uniform rational B-splines basis function (NURBS basis function), and two-dimensional and three-dimensional forms can express the surface and volume:

$$R_{i,j}^{p,q}(\xi,\eta)=\frac{\omega_{i,j}N_{i,p}(\xi)M_{j,q}(\eta)}{\sum_{i=1}^{n}\sum_{j=1}^{m}\omega_{i,j}N_{i,p}(\xi)M_{j,q}(\eta)} \tag{4}$$

$$R(\xi,\eta)=\sum_{i=1}^{n}\sum_{j=1}^{m}R_{i,j}^{p,q}(\xi,\eta)\boldsymbol{B}_{i,j} \tag{5}$$

$$R_{i,j,k}^{p,q,r}(\xi,\eta,\zeta)=\frac{\omega_{i,j,k}N_{i,p}(\xi)M_{j,q}(\eta)L_{k,r}(\zeta)}{\sum_{i=1}^{n}\sum_{j=1}^{m}\sum_{k=1}^{l}\omega_{i,j,k}N_{i,p}(\xi)M_{j,q}(\eta)L_{k,r}(\zeta)} \tag{6}$$

$$R(\xi,\eta,\zeta)=\sum_{k=1}^{l}\sum_{j=1}^{m}\sum_{i=1}^{n}R_{i,j,k}^{p,q,r}(\xi,\eta,\zeta)\boldsymbol{B}_{i,j,k} \tag{7}$$

where *p, q, r* are the orders of basis function; *i, j, k* are the total numbers of basis function; ω are the weights and $\boldsymbol{B}$ are the control points.

2.3. Description of the Coupling System

The IGA is used to describe the displacement field and sound pressure field of the coupling system:

$$w_1(\xi,\eta)=R(\xi,\eta)\mathbf{u}_1=\mathbf{R}_s\mathbf{U}_1 \tag{8}$$

$$w_2(\xi,\eta)=R(\xi,\eta)\mathbf{u}_2=\mathbf{R}_s\mathbf{U}_2 \tag{9}$$

$$p_f(\xi,\eta,\zeta)=R(\xi,\eta,\zeta)\mathbf{p}=\mathbf{R}_f\mathbf{P} \tag{10}$$

where $\mathbf{u}_1$ is the displacement vector of the incident plate, $\mathbf{u}_2$ is the displacement vector of the radiation plate; $\mathbf{p}$ is the sound pressure vector of the acoustic cavity.

On the coupling surface, the force and velocity are continuous, and the weak formula of the governing equations of the double-plate coupling system can be obtained by the variational method:

$$\int_{\Omega_{s1}^h}\delta\sigma^{\mathrm{T}}\varepsilon\mathrm{d}\Omega+\int_{\Omega_{s1}^h}\rho_s\delta\boldsymbol{u}_{s1}\cdot\frac{\partial^2\boldsymbol{u}_{s1}}{\partial t^2}\mathrm{d}\Omega-\int_{\Gamma_{c1}^h}p_f\left(\delta\boldsymbol{u}_{s1}\cdot\boldsymbol{n}_f\right)\mathrm{d}\Gamma=\mathbf{F}_{s1} \tag{11}$$

$$\int_{\Omega_{s2}^h}\delta\sigma^{\mathrm{T}}\varepsilon\mathrm{d}\Omega+\int_{\Omega_{s2}^h}\rho_s\delta\boldsymbol{u}_{s2}\cdot\frac{\partial^2\boldsymbol{u}_{s2}}{\partial t^2}\mathrm{d}\Omega+\int_{\Gamma_{c2}^h}p_f\left(\delta\boldsymbol{u}_{s2}\cdot\boldsymbol{n}_f\right)\mathrm{d}\Gamma=\mathbf{F}_{s2} \tag{12}$$

$$\begin{aligned}&\int_{\Omega_f^h}\nabla\delta p_f\cdot\nabla p_f\mathrm{d}\Omega+\frac{1}{c_f^2}\int_{\Omega_f^h}\delta p_f\ddot{p}_f\mathrm{d}\Omega+\int_{\Gamma_{c1}^h}\delta p_f\left(\rho_f\frac{\partial^2\boldsymbol{u}_{s1}}{\partial t^2}\cdot n_f\right)\mathrm{d}\Gamma\\&-\int_{\Gamma_{c2}^h}\delta p_f\left(\rho_f\frac{\partial^2\boldsymbol{u}_{s2}}{\partial t^2}\cdot n_f\right)\mathrm{d}\Gamma=\mathbf{F}_f\end{aligned} \tag{13}$$

Substituting Equations (8)-(10) into Equations (11)-(13) can obtain the coupling equation of the system:

$$\left\{\begin{bmatrix}\mathbf{K}_{s1} & \mathbf{0} & -\mathbf{C}_{up1}\\ \mathbf{0} & \mathbf{K}_{s2} & \mathbf{C}_{up2}\\ \mathbf{0} & \mathbf{0} & \mathbf{K}_{f}\end{bmatrix}-\omega^{2}\begin{bmatrix}\mathbf{M}_{s1} & \mathbf{0} & \mathbf{0}\\ \mathbf{0} & \mathbf{M}_{s2} & \mathbf{0}\\ \rho_{f}\mathbf{C}_{up1}^{\mathrm{T}} & -\rho_{f}\mathbf{C}_{up2}^{\mathrm{T}} & \mathbf{M}_{f}\end{bmatrix}\right\}\begin{Bmatrix}\mathbf{U}_{1}\\ \mathbf{U}_{2}\\ \mathbf{P}\end{Bmatrix}=\begin{Bmatrix}\mathbf{F}_{s1}\\ \mathbf{F}_{s2}\\ \mathbf{F}_{f}\end{Bmatrix} \quad (14)$$

where $s1$ is the incident plate, $s2$ is the radiated plate; $\mathbf{K}$, $\mathbf{M}$ and $\mathbf{C}$ are the stiffness matrix, mass matrix and coupling matrix respectively, and $\mathbf{F}$ represents the external excitation; ρ_f is air density; ω is angular frequency.

2.4. Sound Transmission Loss

The STL as a crucial metric in the study of noise control, it can be expressed as a ratio of incident power Π_{in} to radiated power Π_r:

$$STL = 10\log_{10}\left(\frac{\Pi_{in}}{\Pi_r}\right) \quad (15)$$

The acoustic excitation of the incident plate is the oblique plane wave with tilt angle φ and azimuth angle θ. The acoustic excitation as the plane wave can be converted into pressure applied to the incident plate:

$$P(x,y,z) = 2P_i \exp(j\omega t - jk_0 z\cos\varphi - jk_0 x\sin\varphi\cos\theta - jk_0 y\sin\varphi\sin\theta) \quad (16)$$

where P_i is the amplitude of the incident wave; k_0 is the wave number, $k_0 = \omega / c_f$; c_f is the sound velocity.

The incident sound power of the system is:

$$\Pi_{in} = \frac{1}{2}Re\iint_A p_i \cdot v_i^* dA \quad (17)$$

where Re denotes the real part; p_i is the sound pressure of the incident wave; v_i is the sound velocity of the incident wave; $*$ is the complex conjugate.

Due to the using of plane wave and the medium is air, the formula will be transformed into:

$$\Pi_{in} = \frac{p_i^2 \cos\varphi \cdot Lx \cdot Ly}{2\rho_f c_f} \quad (18)$$

The sound power of the radiated plate is:

$$\Pi_r = \frac{1}{2}Re\iint_A p_r \cdot v_r^* dA \quad (19)$$

where p_r is the sound pressure; v_r is the sound velocity of the radiated wave.

v_r can be expressed by the displacement of the radiated plate:

$$v_r(x,y) = j\omega \cdot w_2(x,y) \quad (20)$$

Based on Rayleigh integral, the radiated sound pressure and sound power can be expressed as:

$$p_r(x,y) = \frac{jk\rho_{air}c_{air}}{2\pi}\iint_S v_r(x_s,y_s)\frac{e^{-jkr}}{r}dS \quad (21)$$

$$\Pi_r = \frac{\rho_{air}c_{air}}{2}\frac{jk}{2\pi}Re\iint_s\iint_s v_r(x_s,y_s)\frac{e^{-jkr}}{r}v_r^*(x,y)dsds \quad (22)$$

The radiated plate is discretized, and divided into $M \times M$ squares.

The area of each square is S_m:

$$\Pi_r = \sum_{m=1}^{M}\sum_{n=1}^{M} v_{r_m} \frac{\rho_{air} c_{air}}{2} \frac{k^2}{2\pi} (S_m)^2 \frac{\sin(kr_{mn})}{kr_{mn}} v_{r_n}^* \tag{23}$$

where v_{r_m} denotes the vibration velocity of the center of each square; r_{mn} denotes the distance between the center points of each square.

$$\Pi_r = \sum_{m=1}^{M}\sum_{n=1}^{M} v_{r_m} R_{mn} v_{r_n}^* = \left(\mathbf{v}_r\right)^H \mathbf{R}\mathbf{v}_r \tag{24}$$

where $\mathbf{v}_r$ is the column vector of velocity; H denotes conjugate transpose; $\mathbf{R}$ is a real symmetric matrix, and its elements obtained by Equation(25):

$$R_{mn} = \begin{cases} \dfrac{k^2 (\Delta S)^2 \rho_{air} c_{air}}{4\pi} \dfrac{\sin(kr_{mn})}{kr_{mn}} & m \neq n \\ \dfrac{k^2 (\Delta S)^2 \rho_{air} c_{air}}{4\pi} & m = n \end{cases} \tag{25}$$

3. Numerical Examples

This part verifies the accuracy and convergence of isogeometric modeling, based on this, this article study effects of cavity depth and power-law parameter on the STL of the coupling system.

3.1. Verification Analysis

The FG plates are composed of ceramic and aluminum alloy. The material properties of both are shown in **Table 1**. The medium in the acoustic cavity is air. The physical parameters are as follows: sound velocity c_f = 344 m/s, density ρ_f = 1.21 kg/m^3. In particular, the boundary conditions of the two plates in this paper are simple supports. In the acoustic cavity, except for the coupling surfaces, the other four surfaces are rigid.

Table 1. Physical parameters of functionally graded material composition.

	Young's modulus	Density	Poisson's ratio
Ceramic	201.04 GPa	8166 kg/m^3	0.3262
Aluminum alloy	71 GPa	2720 kg/m^3	0.33

To obtain a convergent result for the STL of the system, it is necessary to determine the appropriate order of the basis function and the number of elements. The order and the number of elements divided in each direction of the cavity and the two plates are the same. **Figure 2** is the STL at the order p = {3, 4, 5}, and the number of elements in each direction m = {5, 8, 10, 12}. After comparison, when the order is 4, the elements of each direction is 10, it is enough to achieve the convergence condition.

The size of the two plates is $Lx \times Ly \times t = 0.8\,\text{m} \times 0.7\,\text{m} \times 0.005\,\text{m}$; the size of the acoustic cavity is $Lx \times Ly \times h = 0.8\,\text{m} \times 0.7\,\text{m} \times 0.16\,\text{m}$, the power-law para-

meter $k_x = 1$. The tilt angle $\varphi = \pi/4$ and azimuth angle $\theta = \pi/4$.

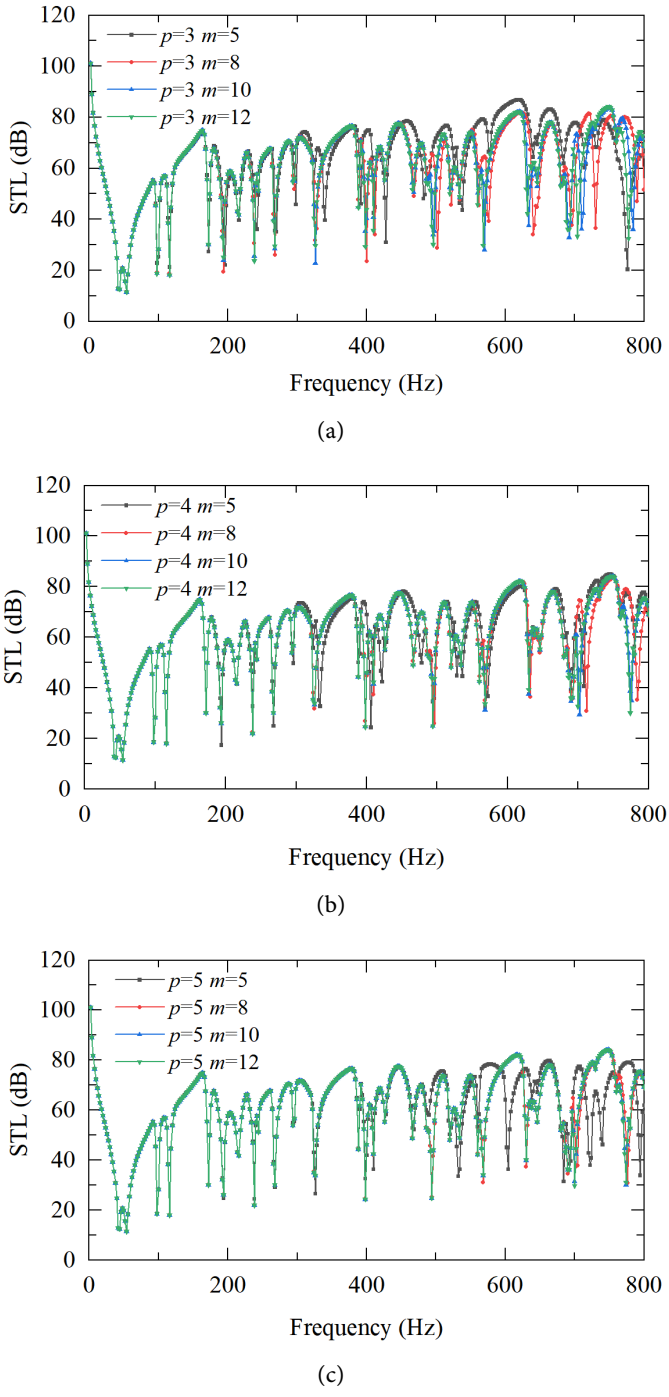

Figure 2. Sound transmission loss corresponding to different order of basis function and element number. (a) $p = 3$; (b) $p = 4$; (c) $p = 5$.

The reliability of isogeometric modeling need be verified, which will be verified by ANSYS. The unit force F is applied at the incident plate (0.24, 0.14, 0.16). The reference value of the decibel is the velocity 10^{-9} m/s, the sound pressure 2×10^{-5} Pa.

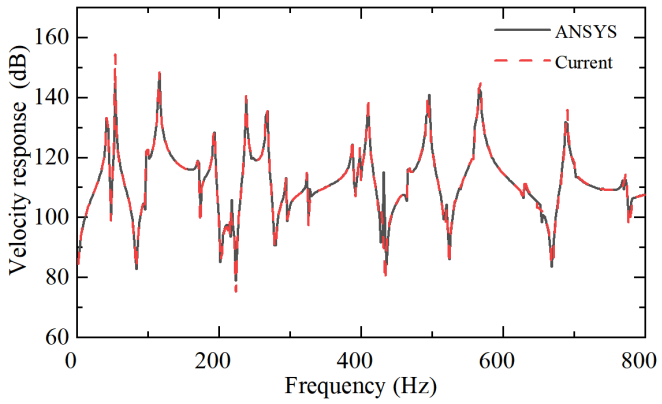

(a)

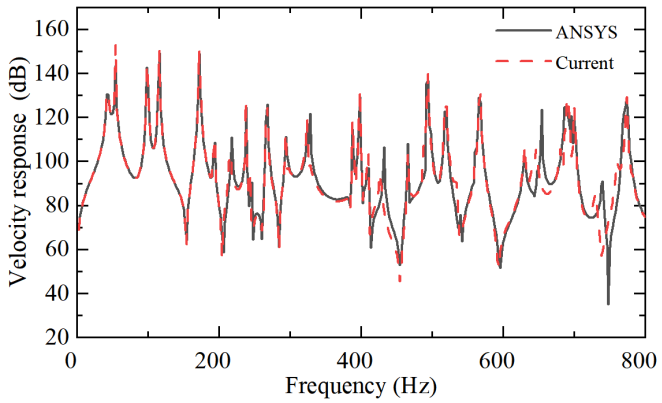

(b)

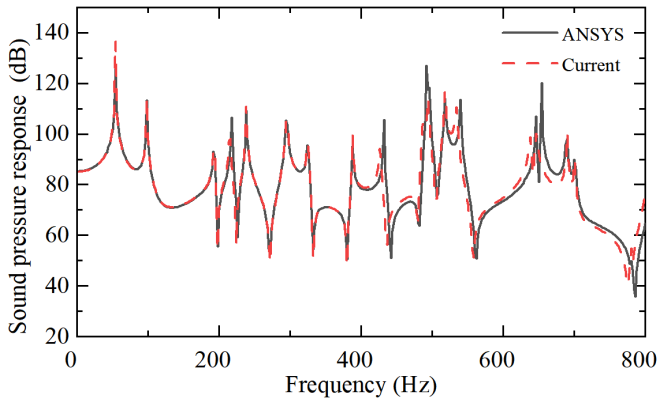

(c)

Figure 3. Response of the coupling system under point force excitation. (a) Velocity response at (0.4, 0.14, 0.16) point on the incident plate; (b) Velocity response at (0.56, 0.49, 0) point on the radiated plate; (c) Sound pressure response at (0.24, 0.35, 0.12) point in the acoustic cavity.

Figure 3 shows the velocity and the sound pressure responses of the system after applying the unit force. It can be seen that both the velocity and the sound pressure responses are basically consistent with ANSYS, indicating that the isogeometric modeling is accurate.

Since the literature on the STL of the coupling systems is limited, FGMs degenerate the power-law parameter $k_x = 0$ and compare it with homogeneous materials of related literature [1] to verify the accuracy. Except that the thickness of the incident plate and the radiated plate is modified to 0.003 m and 0.004 m respectively, other physical parameters remain unchanged.

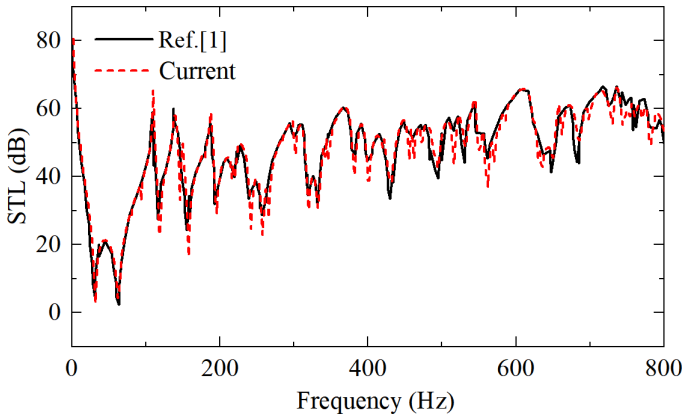

Figure 4. The STL of this current method is compared with literature [1].

Compared with the results solved by IGA in **Figure 4**, the STL curves are still basically consistent, which verifies the reliability of modeling again.

3.2. Parameter Analysis

Next, the influence of key parameters is studied such as cavity depth and power-law parameter on the acoustic radiation of the double plate-cavity coupling system with in-pane FGMs. The material used is the same as the previous section, and the thickness of the plates is 0.005 m.

This part investigates the effect of cavity depth on the STL when the power-law parameter $k_x = 1$. **Figure 5** is the 3D plot of the STL with different cavity thickness. At 0 - 200 Hz, the STL will increase with the increase of the cavity depth; when it is greater than 200 Hz, the cavity depth increases monotonously

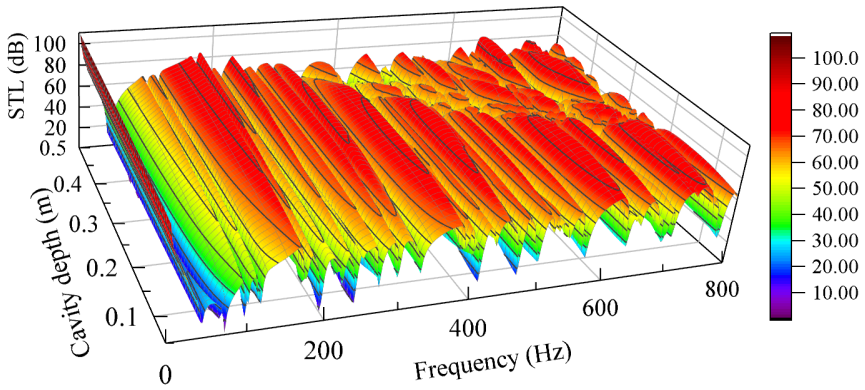

Figure 5. 3D plot of the STL with different cavity depths *h*.

in the range of 0 - 0.2 m, and when it is greater than 0.2 m, it changes irregularly.

Figure 6 is the STL curves with cavity depth h = {0.10 m, 0.15 m, 0.20 m}. Most obviously, as the cavity depth increases, the STL will also increase. In addition, at 200 - 800 Hz, the valleys in the curve are concentrated at the same frequency, indicating that the cavity depth has little effect on the frequency. There will be a certain offset at other frequencies, that is, when 0 - 200 Hz, the cavity depth has a great effect on the frequency.

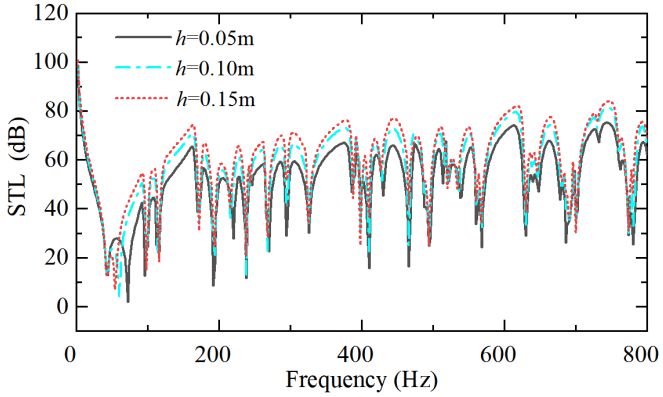

Figure 6. The STL with cavity depths h = {0.05 m, 0.10 m, 0.15 m}.

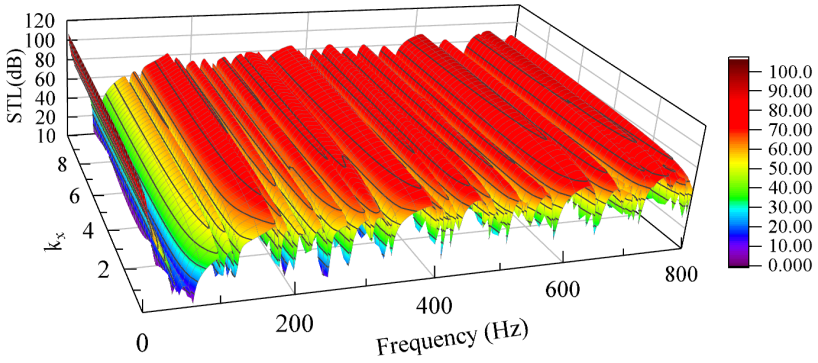

Figure 7. 3D plot of the STL with different power-law parameters k_x.

Finally, the influence of power-law parameter on the STL is studied. **Figure 7** is the 3D plot of the STL with different power-law parameters. The change of STL is very regular. The STL increases with the increase of the power-law parameter, and the increase of k_x = 0 - 4 is larger than that of k_x = 4 - 10. This is because when the power-law parameter increases, the metal content in the FG plates decreases, and when the power-law index is small, the material properties of the FG plates are more affected.

Figure 8 is the STL curve with the power-law parameter k_x = {0, 1, 2} when the cavity depth is 0.16m. As the power-law parameter increases, the STL of the system also increases. In the frequency range of the study, the peaks and valleys of the same order do not appear at the same frequency, and there is a certain de-

gree of deviation, indicating that the power-law parameter has a great influence on the natural frequency of the system.

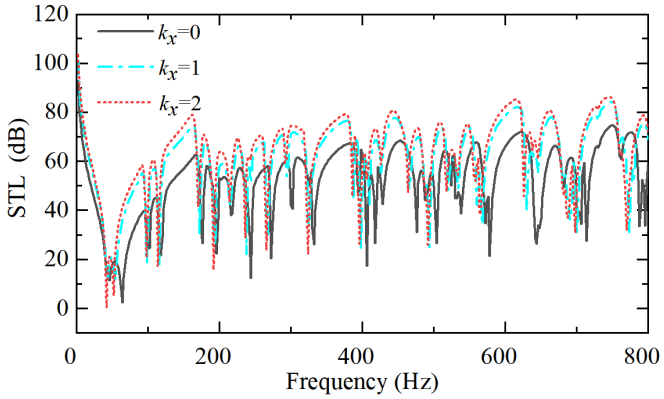

Figure 8. The STL with power-law parameters $k_x = \{0, 1, 2\}$.

4. Conclusions

The acoustic radiation model of the double plate-cavity coupling system with in-plane FGMs is established by IGA. The two-dimensional NURBS basis function and three-dimensional NURBS basis function are used to represent the plates and acoustic cavity, respectively. The accuracy and convergence of this model is verified by ANASYS and literature. On this basis, the influence of power-law parameter and cavity depth on the STL of the coupling system is studied, and the following conclusions are obtained:

1) When the frequency is small, the STL will increase with the increase of the cavity depth. However, at higher frequencies, the relationship between the cavity depth and the STL becomes less regular.

2) As the power-law parameter increases, the STL also exhibits a corresponding increase. In other words, a higher metal content results in a smaller STL, whereas a higher ceramic content leads to a greater STL.

Acknowledgements

The authors acknowledge the financial support from the National Natural Science Foundation of China (No. 52205091).

Conflicts of Interest

The authors declare no conflicts of interest regarding the publication of this paper.

References

[1] Shi, S.X., Jin, G.Y. and Liu, Z.G. (2014) Vibro-Acoustic Behaviors of an Elastically Restrained Double-Plate Structure with an Acoustic Cavity of Arbitrary Boundary Impedance. *Applied Acoustics*, **76**, 431-444. https://doi.org/10.1016/j.apacoust.2013.09.008

[2] Xin, F.X., Lu, T.J. and Chen, C.Q. (2008) Vibroacoustic Behavior of Clamp Mounted Double-Plate Partition with Enclosure Air Cavity. *The Journal of the Acoustical Society of America*, **124**, 3604-3612. https://doi.org/10.1121/1.3006956

[3] Yairi, M., Sakagami, K., Sakagami, E., Morimoto, M., Minemura, A. and Andow, K. (2002) Sound Radiation from a Double-Leaf Elastic Plate with a Point Force Excitation: Effect of an Interior Plate on the Structure-Borne Sound Radiation. *Applied Acoustics*, **63**, 737-757. https://doi.org/10.1016/S0003-682X(01)00075-5

[4] Soleymani, S., Memarzadeh, P. and Toghraie, D. (2023) A Size-Dependent Analytical Model to Predict Sound Transmission Loss of Double-Walled Fiber Metal Laminated Nanoplates. *Mechanics Based Design of Structures and Machines*, **52**, 3358-3388. https://doi.org/10.1080/15397734.2023.2201359

[5] Chandra, N., Raja, S. and Gopal, K.V.N. (2014) Vibro-Acoustic Response and Sound Transmission Loss Analysis of Functionally Graded Plates. *Journal of Sound and Vibration*, **333**, 5786-5802. https://doi.org/10.1016/j.jsv.2014.06.031

[6] Chandra, N., Raja, S. and Gopal, K.V.N. (2015) A Comprehensive Analysis on the Structural-Acoustic Aspects of Various Functionally Graded Plates. *International Journal of Applied Mechanics*, **7**, Article ID: 1550072. https://doi.org/10.1142/S1758825115500726

[7] Yang, T., Huang, Q. and Li, S. (2016) Three-Dimensional Elasticity Solutions for Sound Radiation of Functionally Graded Materials Plates Considering State Space Method. *Shock and Vibration*, **2016**, Article ID: 1403856. https://doi.org/10.1155/2016/1403856

[8] Yang, T., Zheng, W., Huang, Q. and Li, S. (2016) Sound Radiation of Functionally Graded Materials Plates in Thermal Environment. *Composite Structures*, **144**, 165-176. https://doi.org/10.1016/j.compstruct.2016.02.065

[9] Isaac, C.W., Wrona, S., Pawelczyk, M. and Roozen, N.B. (2021) Numerical Investigation of the Vibro-Acoustic Response of Functionally Graded Lightweight Square Plate at Low and Mid-Frequency Regions. *Composite Structures*, **259**, Article ID: 113460. https://doi.org/10.1016/j.compstruct.2020.113460

[10] Fu, T., Chen, Z.B., Yu, H.Y., Hao, Q.J. and Zhao, Y.Z. (2020) Vibratory Response and Acoustic Radiation Behavior of Laminated Functionally Graded Composite Plates in Thermal Environments. *Journal of Sandwich Structures & Materials*, **22**, 1681-1706. https://doi.org/10.1177/1099636219856556

[11] Talebitooti, R., Zarastvand, M. and Rouhani, A.H.S. (2019) Investigating Hyperbolic Shear Deformation Theory on Vibroacoustic Behavior of the Infinite Functionally Graded Thick Plate. *Latin American Journal of Solids and Structures*, **16**, e1391. https://doi.org/10.1590/1679-78254883

[12] Li, B., Zhou, F., Fan, J., Wang, B. and Tan, L. (2023) Research on the Performance Optimization of Turbulent Self-Noise Suppression and Sound Transmission of Acoustic Windows Made from Functionally Graded Material. *Archives of Acoustics*, **48**, 475-495. https://doi.org/10.24425/aoa.2023.146812

[13] Zhou, F., Li, B., Peng, Z., Fan, J. and Wang, B. (2023) Sonar Self-Noise and Acoustic Transmission of Acoustic Window Made from Functionally Gradient Materials. *Acoustics Australia*, **51**, 67-83. https://doi.org/10.1007/s40857-022-00283-4

[14] Chen, M., Jin, G., Ma, X., Zhang, Y., Ye, T. and Liu, Z. (2018) Vibration Analysis for Sector Cylindrical Shells with Bi-Directional Functionally Graded Materials and Elastically Restrained Edges. *Composites Part B*: *Engineering*, **153**, 346-363. https://doi.org/10.1016/j.compositesb.2018.08.129

[15] Ma, H., Zhang, Y. and Yin, X. (2023) Stochastic Response Analysis of 3D Vi-

bro-Acoustic System with Acoustic Impedance and Modeling Parameter Uncertainties. *Applied Mathematical Modelling*, **124**, 393-413. https://doi.org/10.1016/j.apm.2023.08.007

[16] Zhong, S., Jin, G., Ye, T., Zhang, J., Xue, Y. and Chen, M. (2020) Isogeometric Vibration Analysis of Multi-Directional Functionally Gradient Circular, Elliptical and Sector Plates with Variable Thickness. *Composite Structures*, **250**, Article ID: 112470. https://doi.org/10.1016/j.compstruct.2020.112470

[17] Dinachandra, M. and Raju, S. (2017) Isogeometric Analysis for Acoustic Fluid-Structure Interaction Problems. *International Journal of Mechanical Sciences*, **131**, 8-25. https://doi.org/10.1016/j.ijmecsci.2017.06.041

[18] Mi, Y., Zheng, H., Shen, Y. and Huang, Y. (2018) A Weak Formulation for Isogeometric Analysis of Vibro-Acoustic Systems with Non-Conforming Interfaces. *International Journal of Applied Mechanics*, **10**, Article ID: 1850073. https://doi.org/10.1142/S1758825118500734